Functional plasticity in Hsp70 enabled by diverse modes of client binding

Alireza Mashaghi[1*], Sergey Bezrukavnikov[1*], David Minde[1], Anne S. Wentink[2,3], Roman Kityk[2], Beate Zachmann-Brand[2,3], Matthias Mayer[2], Günter Kramer[2,3], Bernd Bukau[2,3], and Sander J. Tans[1]

[1]FOM institute AMOLF, Science Park 104, 1098 XG Amsterdam, the Netherlands.
[2]Center for Molecular Biology of the University of Heidelberg (ZMBH), DKFZ-ZMBH Alliance, Im Neuenheimer Feld 282, D-69120 Heidelberg, Germany.
[3]German Cancer Research Center (DKFZ), Heidelberg, Germany.
*These authors contributed equally to this work.
Correspondence: S.J. Tans (tans@amolf.nl)

The Hsp70 system is a central hub of chaperone activity in all domains of life. Hsp70 performs a plethora of tasks, including folding assistance, protection against aggregation, protein trafficking, and enzyme activity regulation[1-5], and interacts with non-folded chains, as well as near-native, misfolded, and aggregated proteins[6-11]. It is believed that Hsp70 achieves its many physiological roles by binding peptide segments that extend from these different protein conformers within a groove that can be covered by an ATP-driven helical lid[12-16]. However, it has been difficult to test directly how Hsp70 interacts with protein substrates in different stages of folding and affects their structure. Moreover, recent indications of diverse lid conformations in Hsp70-substrate complexes raise the possibility of additional interaction mechanisms[16-19]. Addressing these issues is technically challenging, given the conformational dynamics of both chaperone and client, the transient nature of their interaction, and the involvement of co-chaperones and the ATP hydrolysis cycle[20]. Using optical tweezers, we show that bacterial Hsp70 (DnaK) binds and stabilizes not only extended peptide segments, but also partially folded and near-native protein structures. The Hsp70 lid and groove act synergistically when stabilizing folded structures: stabilization was abolished when truncating the lid and less efficient when mutating the groove. The diversity of binding modes has important consequences: 1) Hsp70 can both stabilize and destabilize folded structures, in a nucleotide-regulated manner. 2) Like Hsp90 and GroEL, Hsp70 can affect late stages of protein folding. 3) Hsp70 can suppress aggregation by protecting partially folded structures as well as unfolded protein chains. Overall, the findings indicate an extension of the Hsp70 canonical model that potentially affects a wide range of physiological roles of the Hsp70 system.

To study the DnaK system at the single-molecule level, we first used an engineered substrate that is prone to misfolding *in vitro*: four Maltose Binding Proteins linked head-to-tail (4MBP, Fig. 1a). Mechanical stretching of 4MBP in the absence of chaperone[21,22] first produced a gradual unfolding of the C-terminal segments of all four MBP proteins (Fig. 1b, N ➔ 4), followed by the distinct unfolding events of the four remaining core structures (Fig. 1b, 4 ➔ 3 ➔ 2 ➔ 1 ➔ U). Relaxation to low forces and a waiting period of 5 s provided an opportunity to refold. However, while subsequent stretching showed a compact structure had formed, these structures typically failed to unfold (termed tight misfold, Fig. 1b) or unfolded in steps larger than one MBP core (termed weak misfold). Isolated 4MBP thus formed small aggregate structures consisting of more than one MBP repeat (Fig. 1c). Next, we performed these experiments in a buffer containing ATP and the DnaK chaperone system (DnaK, DnaJ, GrpE, Fig. 1d, Extended Data Fig. 1-4). Unfolding and relaxation now rarely produced tight misfolds, though weak misfolds still formed (Fig. 1e, f). Moreover, the data showed more unfolding steps corresponding to a single MBP core ($p < 0.05$, Fig. 1e, green arrows), indicating the native-like refolding of core structures. These results show that the DnaK system can promote the correct refolding of a misfolding- and aggregation-prone protein, consistent with previous bulk studies of Hsp70[2,5,14]. However, they do not reveal how the various components of the DnaK system affect client conformations during the different stages of folding.

To understand the underlying mechanisms we focused on the simpler case of single MBP to preclude aggregation and omitted the co-chaperones (Fig. 2a). Multiple protocols were followed: First, we unfolded MBP, which occurred in a two-step manner via the core state[21,22] (Fig. 2b), and then performed cycles of relaxation, waiting at 0 pN for 5 s, and subsequent stretching, all in the absence of chaperones. Stretching indicated the chain either had remained unfolded, or had refolded to a compact structure that typically unfolded in the same two-step manner (Fig. 2b). The refolding probability p_r was about 0.85 (Fig. 2c), which increased for longer waiting periods at 0 pN[21,22]. Second, the cycle was paused at 0 pN, DnaK was flown in and allowed to interact. The DnaK lid is thought to be predominantly open in the presence of ATP and mostly closed after hydrolysis to ADP. We thus used a 1 mM ADP buffer with small amounts (~5%) of ATP (termed ADP loading buffer) in order to stall the ATP cycle after hydrolysis and promote DnaK-MBP binding. Stretching-relaxation cycles were then resumed for the same molecule. Surprisingly, the protein structures now typically failed to unfold over multiple such cycles until the tether broke. The structures sustained high forces (F_u > 40 pN) well above the native unfolding force (22 ± 5 pN), and sometimes even exceeded the effective maximum for our assay (65 pN)[23] (Fig 2d, j).

Notably, this scenario is unlike 4MBP aggregation (Fig. 1b), as aggregation partners are not available here. Instead, the data suggested that in ADP loading buffer, DnaK bound to folded structures and stabilized them against forced unfolding. When MBP molecules were stretched for the first time in the presence of DnaK and ADP loading buffer, they unfolded in similar manner as isolated MBP without DnaK (F_u = 23 ± 4 pN), which indicated that DnaK does not interact with fully native MBP, or only weakly. Rather, the data suggested MBP is in a near-native state when stabilized by DnaK. Specifically, the MBP states stabilized after DnaK flow-in (Fig. 2d) had folded in the absence of chaperones, which yields native-like states (Fig. 2b). The stabilized structures were typically compact like the native or core MBP states, but could also display lengths in between those of the core and unfolded states (Fig. 2d-e). Native MBP could also be stabilized after a minimal perturbation, by unfolding the C-terminal segment in a first pull and then relaxing the force to preserve the native core state (Extended Data Fig. 5b). Overall, these data indicated that DnaK can stabilize partially folded and near-native MBP states against forced unfolding.

Previous work had suggested, however, that DnaK rather stabilizes the unfolded state of substrates (Extended Data Fig. 2, 3, 4)[24]. With the aim to promote this binding mode, we modified the protocol. After a few unfolding-refolding cycles, unfolded MBP was kept at a moderate force to prevent refolding, and incubated for minutes with DnaK and ADP loading buffer. In subsequent relaxation-stretching cycles, MBP now remained unfolded (p_r ~ 0.05; Fig. 2f-g), indicating that DnaK had bound to and stabilized the unfolded chain. Next, we reduced the DnaK incubation time from minutes to seconds by first unfolding MBP in the presence of DnaK and ADP loading buffer, and immediately subjecting it to relaxation and stretching (Extended Data Fig. 5c-d). Unfolded chains now did refold in subsequent cycles. Moreover, the refolded structures typically unfolded at increasingly high forces, until they were locked into a compact state that could not be unfolded (Extended Data Fig. 5d). Consistently, such a compact and locked state was achieved in earlier cycles for longer waiting times at 0 pN (Extended Data Fig. 5e-f). These data suggested a kinetic partitioning: unfolded chains can be bound by DnaK[25], which blocks their refolding, unless the chains fold first (folding time is about 1 s for MBP)[21], and are then stabilized by DnaK in a folded state.

The observed stabilization by DnaK also occurred during active ATP hydrolysis. In the presence of DnaK and 1 mM ATP, we found that refolded structures frequently unfolded via partially folded structures smaller than the core state (44% of the traces, lifetime of partial structure τ = 1.1 ± 0.6 s, Fig. 2h-i). For example, the light green curve in Fig. 2h displayed a partially folded structure beyond 5 pN that was stable for τ ~ 4 s, and then unfolded fully at 30 pN. This observation suggested the folded structure was stabilized by DnaK, and then unfolded when DnaK was released as it progressed

through the ATP cycle. Consistently, the occurrence of transiently stable partial folds was higher than without chaperones ($p < 0.01$, 8% of the traces, $\tau \sim 0.5$ s), but lower than with DnaK and ADP loading buffer ($p < 0.01$, all traces, τ up to 150 s). The stabilization of extended and folded states by DnaK was also observed at lower DnaK concentrations (Fig. 2d, f, Extended Data Fig. 5g), and in presence of HPLC purified (ATP free) ADP (Extended Data Fig. 5h-i). Consistently, stabilization was not observed for a DnaK mutant (T199A) that is trapped in the open ATP state (Fig. 2j, Extended Data Fig. 5j-k). Overall, these results indicated that stabilization of partially folded structures by DnaK is modulated by its ATP hydrolysis cycle.

Which structural elements of the Hsp70 substrate-binding domain are conducive to stabilizing folded MBP conformations? The helical lid may play a role, as implied by the observation that ATP affects both binding to folded structures (Fig. 2d, h) and lid conformation[17], but this evidence is indirect. To address this issue more directly, we investigated DnaK with a truncated lid (DnaK(2-538), Extended Data Fig. 6)[25]. In the presence of this variant and ADP loading buffer, refolded MBP molecules did not show stabilization but rather native-like core unfolding, whether the waiting time at 0 pN was 5 s (F_u = 22 ± 5 pN, Fig. 3 a and e) or minutes (F_u = 24 ± 7 pN, Extended Data Fig. 5l). In contrast, stabilization was observed after minute-long exposure at 0 pN to a DnaK variant that has a mutated binding groove but retains the lid (DnaK-V436F, Fig. 3c). Unfolding then occurred at forces up to 65 pN (Fig. 3c and e), and often (52% of the traces) via partial folds that are only scarcely observed without chaperone[22]. The unfolding forces were lower than for *WT* DnaK however ($p < 0.01$, Fig. 3e). This groove-mutation is reported to reduce peptide affinity by more than 10-fold[25]. Consistent with such a peptide-binding defect, we found that after minute-long exposure to groove-mutated DnaK in the extended state, MBP chains formed folded structures when relaxed to 0 pN for 5 s (N = 13), while refolding was efficiently blocked in the *WT* DnaK exposure experiments (Fig. 2f-g). Lid-truncated DnaK on the other hand, which retains the *WT* groove, was found to suppress refolding in regular stretch-relax cycles ($p < 0.01$, Fig. 3a-b). Thus, the stabilization of folded structures by DnaK is abolished by truncating the lid and weakened by mutating the groove.

We surmised that binding partially folded structures could help to suppress aggregation[27,9,10] (Fig. 1e and 1f). If so, groove-mutated DnaK should retain some of this capability, as it binds folded structures (Fig. 3c). We found that the presence of groove-mutated DnaK and 1 mM ATP indeed decreased tight aggregation of 4MBP ($p < 0.01$, Fig. 3g, Extended Data Fig. 7). The aggregated structures that did form, unfolded at lower forces ($p < 0.01$, Fig. 3h). These findings are consistent with models where DnaK can destabilize misfolded structures[4]. The results may appear paradoxical: how can DnaK both result in more (Fig. 2d) and less (Fig. 3h) stable structures? The ATP-driven DnaK cycle offers a

possible rationale. First, one notes that DnaK stabilizes in the ADP state, and hence only transiently. Moreover, by binding less-stable structures early after relaxation, DnaK can limit more stable structures that would form later (Fig. 4a). Indeed, aggregates may have different structure and be less stable when formed with DnaK present. DnaK may also discriminate between native and non-native structures, and directly destabilize the latter[4]. We find DnaK selectively stabilizes partial and not fully folded MBP, though DnaK selectivity may go further. Overall, the data indicate aggregation can be suppressed by the transient stabilization of (partially) folded structures.

Other components of the DnaK system may also contribute to limiting aggregation. With the full DnaK system present, tight aggregation was less frequent than for DnaK and ATP, though the difference was not large ($p < 0.01$, Fig. 3g). The co-chaperone GrpE did not display any substrate interactions by itself (Extended Data Fig. 8e). In contrast, DnaJ alone completely abolished aggregation (Extended Data Fig. 8b), but blocked refolding as well (Extended Data Fig. 8d). Within the full DnaK chaperone system, the holdase activity of DnaJ did not dominate, as efficient refolding was observed (see Fig. 1e and 1f). These findings thus support previous observations that with ATP and GrpE, DnaK can promote DnaJ release from substrate[26].

Finally, the observations led us to speculate that DnaK could preserve protein structure and function under heat stress. As DnaK unfolds at lower temperatures than MBP, the latter is unsuitable. We instead investigated a monomeric variant of the replication initiation protein RepE (RepE54, Extended Data Fig. 4d), a well-established DnaK substrate[27], using tryptophan fluorescence. We found that with (tryptophan-free) DnaK and ADP, the apparent thermal stability of RepE54 increased by about 5°C (Extended Data Fig. 9). This upshift was not observed for DnaK and ATP or for lid-truncated DnaK with ADP, consistent with central roles for the ADP state and the lid in the stabilization of folded states. Groove-mutated DnaK with ADP also did not show an upshift, suggesting the groove was more important here than in the single-molecule MBP experiments, or limited sensitivity. We further observed that DnaK suppressed the temperature-induced decrease of Luciferase (Extended Data Fig. 4c) activity in the presence of ADP, whereas the ADP buffer alone did not (Extended Data Fig. 10). Together, these data suggested DnaK can stabilize protein structure and activity during heat stress when ATP abundance is limited[5].

From these experiments on DnaK, a picture emerges of an Hsp70 functional repertoire that is broader than previously assumed (Fig. 4b): 1) Hsp70 not only binds extended peptides[4,16,17,28], but also directly binds (partially) folded structures. The Hsp70 lid is central and could adopt reported open conformations[16-18,20] to accommodate and bind folded structures, though indirect action cannot

be excluded, while the groove also conveys stability. 2) In the canonical model, protein chains fold autonomously after Hsp70 release, and can subsequently be transferred to other chaperones that act in later stages, such as Hsp90 and GroEL[11,15]. Our findings suggest Hsp70 can also guide and organize late stages of folding[19], for instance by limiting inter-domain contacts[22], and may not fully release protein substrates until near native. 3) Hsp70 can protect partially folded structures against aggregation in addition to extended peptide segments[29]. 4) Hsp70 is known to destabilize (mis)folded protein structures[4]. Hsp70 could achieve this role by interacting directly with misfolded and aggregated structures. Furthermore, our data show that Hsp70 can also do the opposite, and stabilize partially folded protein structures. These contrasting effects may be controlled by ADP abundance and co-chaperones, which can for instance modulate the lifetime of the ADP state. 5) The findings suggest Hsp70 can preserve enzymatic functions during stress at low energy costs, in line with the reduced energy availability in episodes of stress.

These Hsp70 functions could have important consequences for our understanding of normal cellular physiology as well as pathophysiology. Hsp70 may transfer clients to other chaperones[9,10] without requiring (local) unfolding, and contribute to an evolutionary capacitor role by stabilizing substrate proteins[30]. Co-factors such as HIP[31] that promote the ADP state could play a role in regulating client stabilization. Finally, Hsp70 could control signaling pathways[7] by interacting directly with the folded parts of transcription factors, kinases, and receptors, in addition to their unfolded segments[1,3].

FIGURES

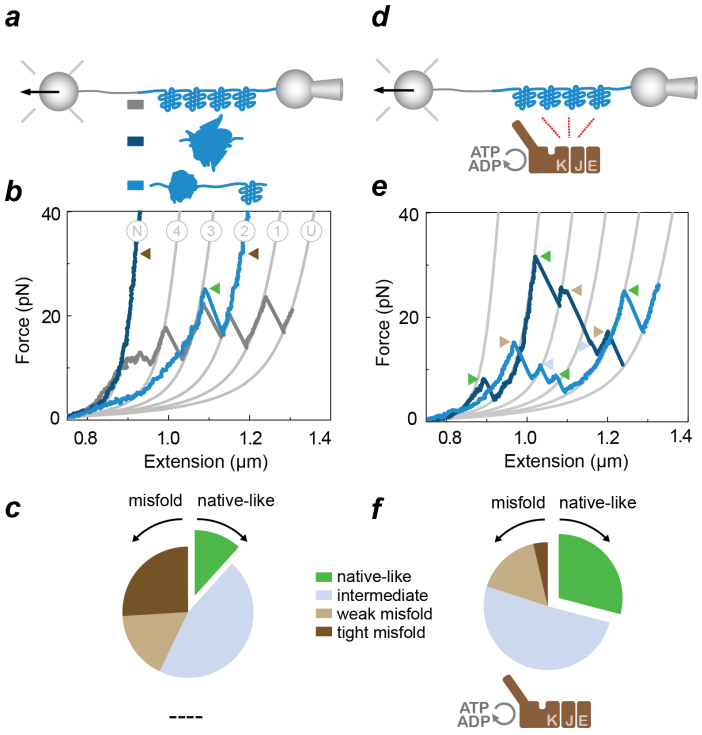

Figure 1 | DnaK chaperone system suppresses aggregation and promotes refolding. **a,** Schematic diagram of the experiment. Protein construct of 4 MBP monomers (4MBP, blue) is attached to a DNA linker (grey) and tethered between two beads[21]. **b,** 4MBP in the absence of chaperones. Thick grey line: First stretching curve showing native 4MBP unfolding. Dark and light blue: subsequent stretching curves corresponding to different types of misfolded states. Triangles: types of events or states (see panel c and f and main text). Thin grey lines: theoretical compliance of DNA-protein construct in states ranging from native (N) to fully unfolded (U). Numbers indicate the number of folded core structures. **c,** Corresponding event fractions (*N* = 38). Intermediate: unfolding events with unfolded length shorter than one MBP core. **d,** Schematic diagram of the experiment. **e,** Stretching curves of 4MBP in the presence of the DnaK system and ATP. **f,** Corresponding event fractions (*N* = 55).

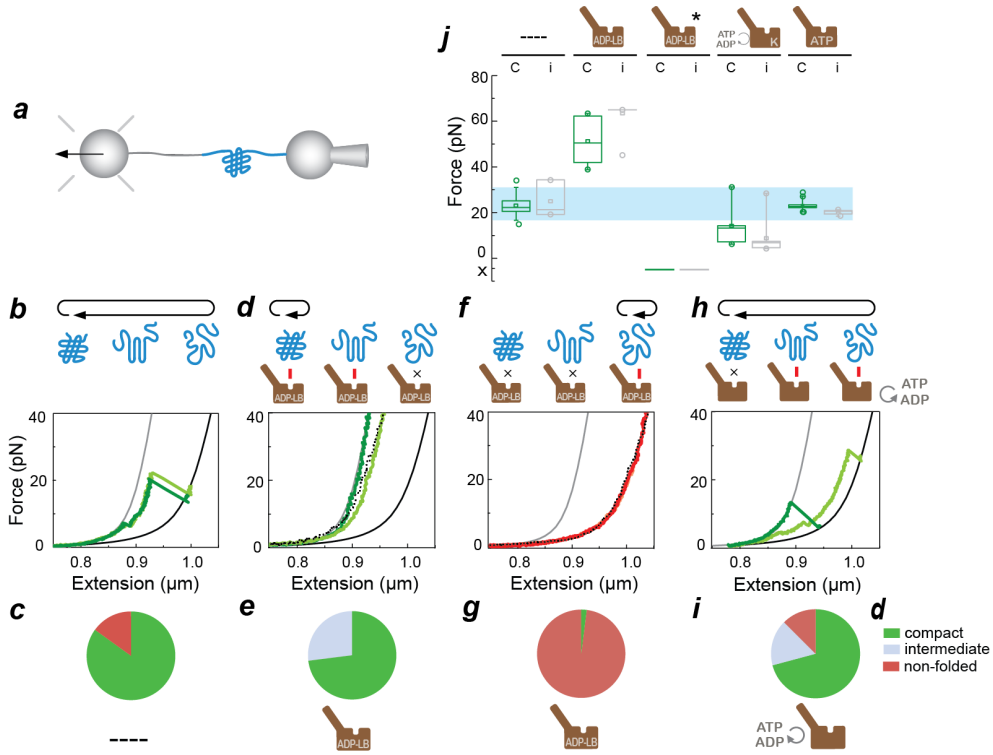

Figure 2 | DnaK binds and stabilizes folded structures in a nucleotide-dependent manner. a, Schematic diagram for single MBP experiments. **b-c,** Stretching of MBP that was unfolded and relaxed in isolation (*N* = 50). **d-e,** Stretching of MBP that was unfolded and relaxed in isolation and then incubated at low force with 1 μM DnaK, 1 mM ADP, and small amounts of ATP (5%), termed ADP loading buffer (ADP-LB, *N* = 35). Dotted line: similar experiment with 100 nM DnaK. **f-g,** Stretching of MBP that was incubated in the unfolded state with 1 μM DnaK and ADP loading buffer and then relaxed (*N* = 15). Dotted line: similar experiment with 100 nM DnaK. **h-i,** Stretching of MBP that was unfolded and relaxed with DnaK and ATP (*N* = 24)**.** Pie charts: states observed after waiting period at 0 pN. Distinguished are compact (native or core-like), intermediate states with length between core and unfolded, and unfolded states. Top cartoons represent these same states and observed transitions between them. Grey and black lines in force-extension graphs: theoretical compliance of tether with fully folded and unfolded MBP respectively. **j,** Unfolding forces corresponding to data in panels b, d, f, and h. Last column is data for DnaK mutant T199A, which traps DnaK in the ATP state in an ATP buffer (Extended Data Fig. 5 j-k; *N* = 18). Star indicates MBP was unfolded when incubated (see panel f), 'c' is core state, 'i' is intermediate state. Cross at force axis: folded structures were not observed. Blue band: the force range of MBP core unfolding without chaperones. Whiskers indicate the 90% and 10% extrema. The band inside the box indicates the median, the rectangle inside the box indicates the mean.

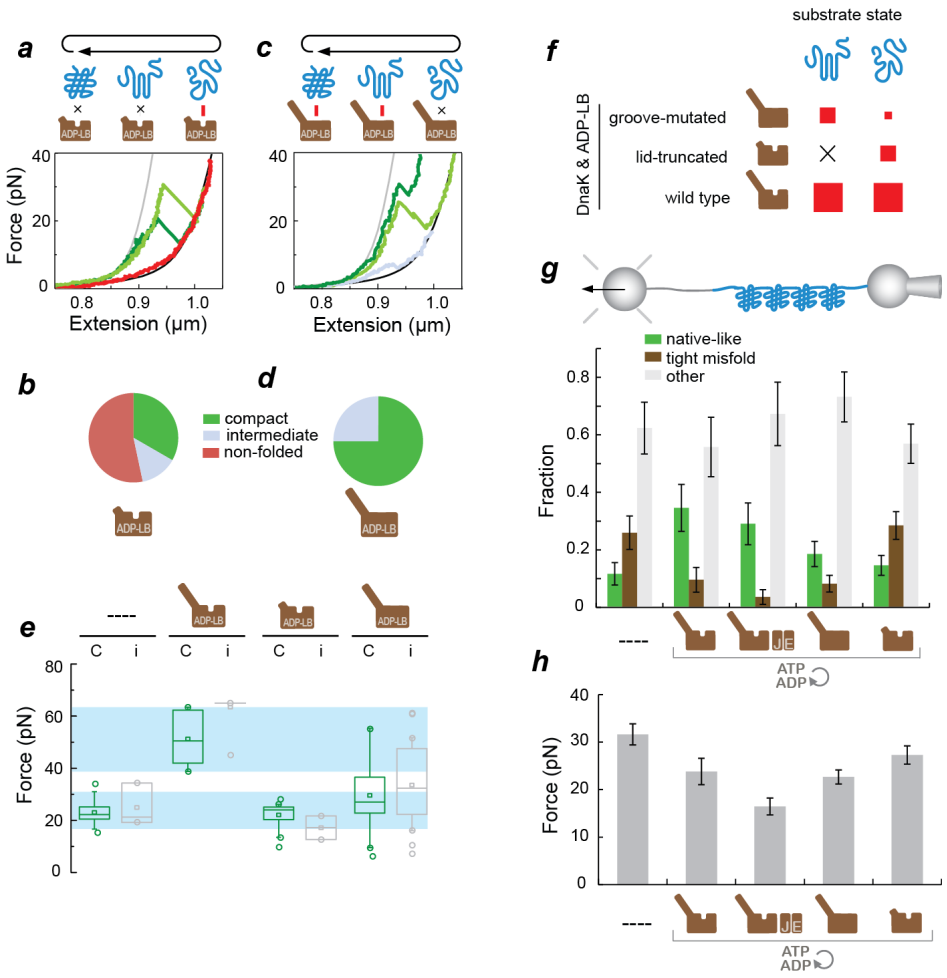

Figure 3 | DnaK lid is central to stabilizing folded structures and suppressing aggregation. **a-b,** Stretching of MBP that was unfolded and relaxed with lid-truncated DnaK(2-538) in ADP loading buffer (ADP-LB, *N* = 15). Waiting time at 0 pN is 5 s. **c-d,** Stretching of MBP that was unfolded and relaxed with groove-mutated DnaK-V436F in ADP loading buffer (*N* = 21). Waiting time at 0 pN is of the order of minutes. Pie charts: states observed after waiting period at 0 pN. Distinguished are compact (native or core-like), intermediate states with length between core and unfolded, and unfolded states. Top cartoons represent these same states and observed transitions between them. **e,** Corresponding unfolding forces. Blue bands: core unfolding force range of MBP in isolation and with DnaK and ADP. 'c' is core state, 'i' is intermediate state. Whiskers indicate the 90% and 10% extrema. The band inside the box indicates the median, the rectangle inside the box indicates the mean. **f,** Red squares qualitatively indicate observed stabilization of folded and extended states by DnaK variants. **g,** Refolding statistics in 4MBP with different DnaK variants. Indicated is the type of event, as a fraction of the total number of events. Error bars are ±1 s.d. **h,** Mean unfolding force of non-native structures formed during 4MBP refolding. Error bars are ±1 s.e.m..

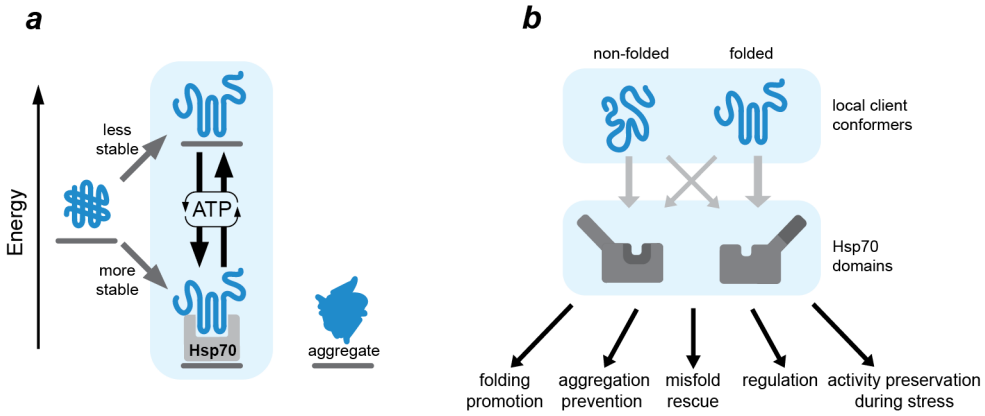

Figure 4 | Model of Hsp70 chaperone action. a, Hsp70 effect on substrate stability. Hsp70 binding can transiently stabilize partially folded structures that are less stable than complete folds upon Hsp70 release. Hsp70 binding can suppress the formation of permanently stable aggregates. ATP abundance and chaperone cofactors provide control of the Hsp70 binding and release, and hence the stabilizing effect of Hsp70. For instance, high ADP and low ATP levels or low nucleotide exchange rates observed with heat-denatured nucleotide exchange factor GrpE[32] or presence of Hip in mammalian cells[31] can prolong Hsp70-mediated stabilization. Hsp70 could bind and (de)stabilize certain structural motifs selectively. **b,** Roles of Hsp70 domains. Hsp70 mediated stabilization of unfolded chains is suppressed by mutating the groove, while the stabilization of folded structures is abolished by truncating the lid, and weakened by mutating the groove. This diversity of binding modes, and ability to not only destabilize but also stabilize folded structures, potentially affects a diverse range of physiological roles of the Hsp70 system.

METHODS

Expression and purification of MBP and 4MBP

N-terminally biotinylated MBP and 4MBP C-terminally fused with 4 Myc tag sequences were produced in *E. coli* as hybrid proteins consisting of an N-terminal Ulp1-cleavable N-terminal His_{10}-SUMO sequence followed by an AviTag sequence (Avidity, LCC, Aurora, Colorado, USA), facilitating *in vivo* biotinylation and four consecutive C-terminal Myc-tag sequences. Proteins were purified from *E. coli* BL21(DE3) cells harboring pBirAcm encoding the biotin ligase (Avidity, LCC, Aurora, Colorado, USA). For over-expression over-night cultures were diluted 1:100 in fresh LB medium supplemented with 20 mg/l Biotin, 20 mg/l Kanamycin, 10 mg/l Chloramphenicol, 0.2% glucose and incubated under vigorous shaking at 30°C. Expression was induced at OD_{600}= 0.6 by addition of 1 mM IPTG for 3 h. Cells were chilled, harvested by centrifugation, flash-frozen in liquid nitrogen and stored at -70°C. Cell pellets were resuspended in ice-cold buffer A (20 mM Tris-HCl pH 7.5, 0.2 M NaCl, 1% Triton X-100, 1 mM PMSF) and lysed using a French Pressure Cell. The lysate was cleared from cell debris by centrifugation at 35.000 g for 30 min and incubated with Ni-IDA matrix (Protino; Macherey-Nagel, Düren, Germany) for 30 min at 4°C. The matrix was washed extensively with buffer A and bound hybrid proteins were eluted in buffer A containing 250 mM imidazole. The eluate was supplemented with His6-Ulp1 protease and dialyzed overnight at 4°C in buffer D (20 mM Tris-HCl pH 7.5, 0.2 M NaCl). Following dialysis coupled with Ulp1 digestion, His6-Ulp1 protease and the His_{10}-SUMO fragment were removed by incubation with Ni-IDA matrix. The unbound fraction containing cleaved MBP or 4 MBP was then loaded on Amylose resin (New England Biolabs) previously equilibrated in buffer D, washed with cold buffer D and bound proteins were eluted in buffer D supplemented with 20 mM maltose. Elution fractions were dialyzed three times for 2 hours at 4°C in 100-fold excess volume of buffer S (20 mM Tris-HCl pH 7.5, 0.2 M NaCl, 1 mM EDTA). 4 MBP purifications in addition were subjected to size-exclusion chromatography using a HiLoad 16/600 Superdex prep grade column. Purified proteins were concentrated using Vivaspin centrifugal concentrators, aliquoted, flash frozen in liquid nitrogen and stored at -70 °C.

Biotinylated proteins were also produced as follows. Purification of MBP and 4MBP containing one N-terminal cystein was performed as described[21]. For biotinylation the purified proteins were dialyzed in buffer B (20 mM Tris-HCl pH 7.5, 0.2 M NaCl, 1 mM EDTA) and incubated on ice for 15 min in buffer B containing 5 mM TCEP to reduce disulfide bonds. A ten-fold molar excess of Maleimide-PEG11-Biotin (Thermo Scientific) dissolved in DMSO was added and biotinylation was performed for 2 hours at 25 °C. Proteins were concentrated and subjected to size-exclusion chromatography using a HiLoad 16/600 Superdex prep grade column. Purified fractions were analyzed by SDS-PAGE, pooled, aliquoted, flash frozen in liquid nitrogen and stored at -70 °C.

WT and mutant chaperones expression and purification

All proteins were produced in *E. coli* from expression plasmids. Wild-type DnaK, DnaK(2-538) (lid-truncated), and DnaK-V436F (groove-mutated) were produced in a *ΔdnaK* strain and purified by ammonium sulfate precipitation, anion exchange chromatography (DEAE-sepharose), ATP-agarose affinity chromatography, gel filtration and strong anion exchange chromatography (Resource Q) as described earlier[33]. DnaJ was purified by chromatography on cation exchange and hydroxyapatite material. GrpE was expressed in a *ΔdnaK* strain and purified by chromatography on DEAE-Sepharose, hydroxyapatite and Superdex 200 as described[34] Tryptophan-free DnaK mutants (W102F) were expressed with an N-terminal His_{10}-SUMO sequence and purified by Ni affinity chromatography, Ulp1 digestion and a second Ni-affinity chromatography step.

Luciferase activity protection assay

Luciferase (80 nM in 40 mM HEPES/KOH pH 7.5, 50 mM potassium acetate, 5 mM magnesium acetate, 2 mM DTT) was incubated in the absence or presence of ATP (2 mM), ADP (3.2 µM), DnaK wild-type or mutant proteins (800 nM), DnaJ (160 nM) and GrpE (400 nM) at 37°C. Luciferase activity was determined by diluting 1 µl aliquots into 124 µl assay buffer (100 mM potassium phosphate (pH 7.8), 25 mM glycylglycine (pH 7.4), 100 mM potassium acetate, 15 mM magnesium acetate, 5 mM ATP), mixing with 125 µl luciferin (80 µM in assay buffer) and monitoring bioluminescence for 5 s without delay using a Biolumat (Berthold).

RepE54 thermal unfolding assay

RepE54 (2 µM in 50 mM HEPES/KOH pH 7.5, 50 mM KCl, 5 mM $MgCl_2$, 2 mM DTT) was incubated at 25°C in the absence or presence of ATP (2 mM), ADP (2 mM), ADP loading buffer conditions (2 mM ADP + 5% ATP), tryptophan-free DnaK wild-type or mutant proteins (2 µM) for 30 min. The unfolding transition of RepE54 was then monitored by fluorescence emission at 329 nm (excitation at 295 nm) as a function of temperature (temperature gradient from 25-65 °C at a rate of 90 °C/hour) on a Jasco FP-6500 spectrofluorometer.

Optical tweezers assay

Anti-digoxigenin (anti-Dig) coated beads (DIGP-20-2, diameter 2.1 mm) were purchased from Spherotech and stored at 4 °C until use. 2553 base pairs DNA handles were prepared and functionalized with digoxigenin (Dig) and biotin at 5'-ends of both strands as described[21]. DNA-coated microspheres were made by mixing ~70 ng of biotin–dsDNA–Dig and 4 µl Dig-coated beads in 10 ml HMK buffer (50 mM HEPES, pH 7.5, 5 mM MgCl2, 100 mM KCl). After a 30 minute incubation on a rotary mixer (4 °C), 1 µl of neutravidin solution (1% w/v) was added to the mixture and incubated at 4°C for 10 more minutes. Next, the unbound neutravidin was washed away by centrifugation, and the beads were dissolved in 400 µl HMK buffer for use in optical tweezers experiments. Carboxylated polystyrene beads (CP-20-10, diameter 2.1 µm, Spherotech) were covalently attached to anti-Myc antibody (Roche Diagnostics) via carbodiimide reaction (Poly-Link Protein Coupling Kit, Polysciences Inc.). Briefly, the beads were washed and then mixed with freshly prepared 1-ethyl-3-(3-dimethylaminopropyl) carbodiimide and the antibody, and mixture was incubated for 3 hours. MBP-coated beads were made by mixing 5 µl of 50 µM solution of either 1MBP or 4MBP and 2 µl Myc-coated beads in 10 µl HMK buffer and incubating the mixture for 30 minutes on a rotary mixer at 4°C. Subsequently, the beads were dissolved in 400 µl HMK buffer for use in optical tweezers experiments.

Optical tweezers assays, buffer contents: Fig. 1b,c: no chaperones; Fig. 1e,f: 100 nM DnaK, 100 nM DnaJ, 50 nM GrpE, 1 mM ATP; Fig. 2b,c: no chaperones; Fig. 2d-g: 1 µM DnaK, 1 mM ADP loading buffer; Fig. 2h,i: 100 nM DnaK, 1 mM ATP; Fig. 3a,b: 1 µM DnaK lid-truncated, 1 mM ADP loading buffer; Fig. 3c,d: 1 µM DnaK groove-mutated, 1 mM ADP loading buffer; Extended Data Fig. 5b: 100 nM DnaK, 1 mM ADP loading buffer; Extended Data Fig. 5c-f: 1 µM DnaK, 1 mM ADP loading buffer; Extended Data Fig. 5g: 100 nM DnaK, 1 mM ADP loading buffer; Extended Data Fig. 5h-i: 1 µM DnaK, 100 µM ADP purified by HPLC; Extended Data Fig. 5j-k: 100 nM DnaK T199A, 1 mM ATP; Extended Data Fig. 5l: 1 µM lid-truncated DnaK and 1 mM ADP loading buffer; Extended Data Fig. 7b: 100 nM DnaK, 1 mM ATP; Extended Data Fig. 7c: 100 nM DnaK lid-truncated, 1 mM ATP; Extended Data Fig. 7d: 100 nM DnaK groove-mutated, 1 mM ATP; Extended Data Fig. 8b: 1 µM DnaJ; Extended Data Fig. 8c: 100 nM DnaJ; Extended Data Fig. 8d: 1 µM GrpE. Number of events (high force): N = 38 (Fig. 1b,c), 55 (Fig. 1e,f), 52 (Extended Data Fig. 7b), 131 (Extended Data Fig. 7c), 96 (Extended Data Fig. 7d). Number of events (low force): N = 50 (Fig. 2b,c), 35 (Fig. 2d,e), 15 (Fig. 2f,g), 24 (Fig. 2h,i), 15 (Fig. 3a,b), 21 (Fig. 3c,d), 6 (Extended Data Fig. 5b), 10 (Extended Data Fig. 5c,d), 11 (Extended Data Fig. 5e,f), 17 (Extended Data Fig. 5g,h), 15 (Extended Data Fig. 5i,j), 4 (Extended Data Fig. 8b), 9 (Extended Data Fig. 8c), 10 (Extended Data Fig. 8d). ADP loading buffer was prepared by dissolving ADP sodium

salt (A2754, Sigma Aldrich) in HMK buffer. The ATP fraction in this buffer was ~5%, as measured by HPLC.

Stretching experiments were performed at room temperature using a custom made optical tweezers setup[18]. MBP-coated bead was trapped in the optical trap and then transferred to a micropipette tip, and, subsequently, DNA-coated bead was trapped. Next, two beads were brought in close contact, allowing a tether between the beads to form. When the micropipette is moved away from the trap, the tether experiences a stretching force, leading to its extension and deflection of the trapped bead from the trap center. Specific tethering to natively folded MBP molecules was detected by the typical two-step unfolding upon stretching. Tethers that broke at low force or showed no unfolding, for instance because of non-specific binding of the neutravidin at the end of the DNA tether to the bead surface, were excluded. The deflection is monitored by collecting the transmitted laser light and directing it to quadrant photodiode where it is recorded at 50 Hz. The data is filtered with 5th order Butterworth filter at 20 Hz prior to saving. Trap stiffness and sensitivity were measured to be 169 ± 24 pN/um and 2.74 ± 0.24 V/um correspondingly. A nanopositioning piezo stage is used to move the flow chamber and micropipette at a speed of 50 nm/s that corresponds to a pulling rate on the tethered MBP construct of ~5 pN/s at unfolding. Differences between pie charts were analyzed using one-tailed two-proportion z-test. Statistical analysis of sustained forces in different conditions was performed using the Kruskal-Wallis (one-way ANOVA on ranks) test, given that the forces are not distributed normally and have non-equal variances for different groups. Test results such as *p* values are reported in the main text.

EXTENDED DATA

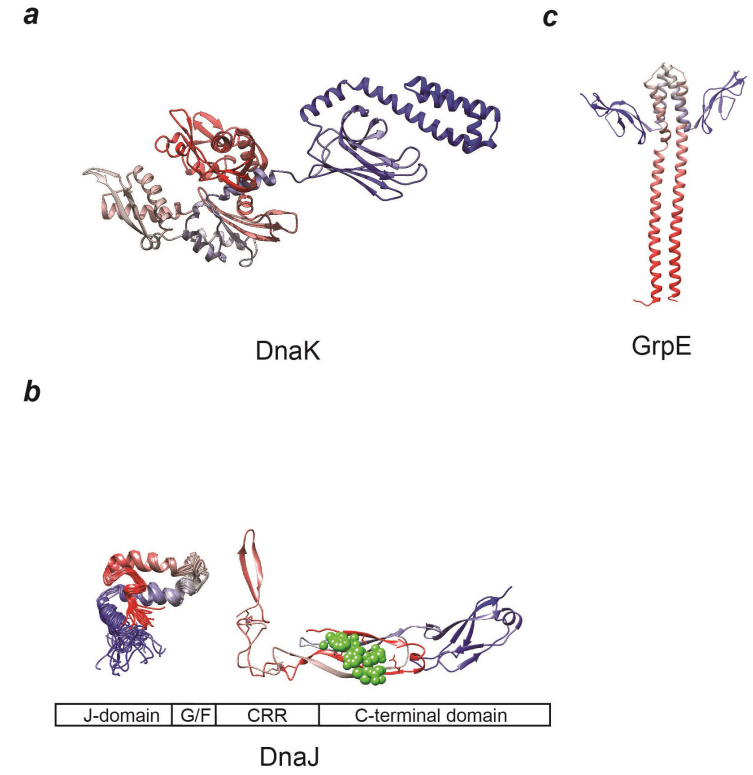

Extended Data Figure 1| Domain architectures of DnaK, DnaJ and GrpE.
a, Structure of *E. coli* DnaK bound to peptide substrate and ADP nucleotide (PDB 2KHO) in N-to-C terminal color gradient from red (N-terminus) over dark grey to blue (C-terminus) [ref 33]. **b,** DnaJ domain structure containing J-domain, Glycine/Phenylalanine-rich domain (G/F), Cysteine-Rich Region/Zn finger (CRR) and C-terminal domain; partial NMR structures of J domain (PDB ID: 1XBL) and crystal structure comprising cysteine-rich domain (CRR) and peptide binding domain of the yeast homolog with co-crystalized peptide substrate highlighted in green spheres (PDB ID: 1NLT)[35,36]. **c,** GrpE structure (PDB ID : 1DKG)[37].

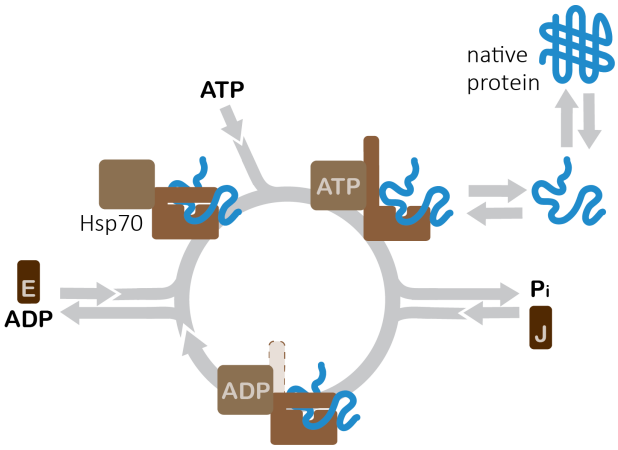

Extended Data Figure 2| Canonical nucleotide-driven cycle of Hsp70-client interactions.
Hsp70 is known to interact with a large range of protein conformations from unfolded nascent chains over near-native proteins to aggregates and misfolded states. Non-native protein conformers are

captured via short extended peptide segments by the substrate-binding groove of Hsp70. Hsp40 (DnaJ) then accelerates the ATP hydrolysis reaction together with bound substrate. Hsp70-ADP locks the substrate under the closed helical lid of the substrate-binding domain in the 'high-affinity' state. The lid could also adopt the open conformation according to recent indications [refs 16-18, 20]. Nucleotide Exchange Factor (GrpE) subsequently accelerates the release of ADP and either spontaneous fluctuations of the lid or new ATP molecules facilitate the release of the substrate to regenerate Hsp70-ATP for another round of the cycle (adapted from ref. [38]).

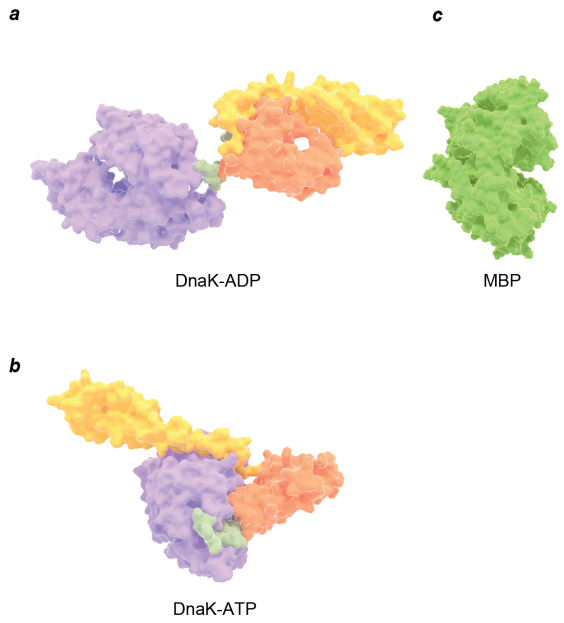

Extended Data Figure 3| Protein structures.
a, DnaK in ADP state (PDB code: 2KHO). Domain boundaries indicated in different colors: nucleotide binding domain (purple, 1-383), hydrophobic linker (green, 384-396), β-sheet subdomain of substrate binding domain with groove (orange, 397-502), α-helical lid subdomain of substrate binding domain (yellow, 503-602)[39]. **b,** DnaK in ATP bound open conformation (PDB code: 4B9Q). **c,** apo MBP (PDB code: 2MV0). Proteins are displayed in the same scale to aid visualizing interactions between them.

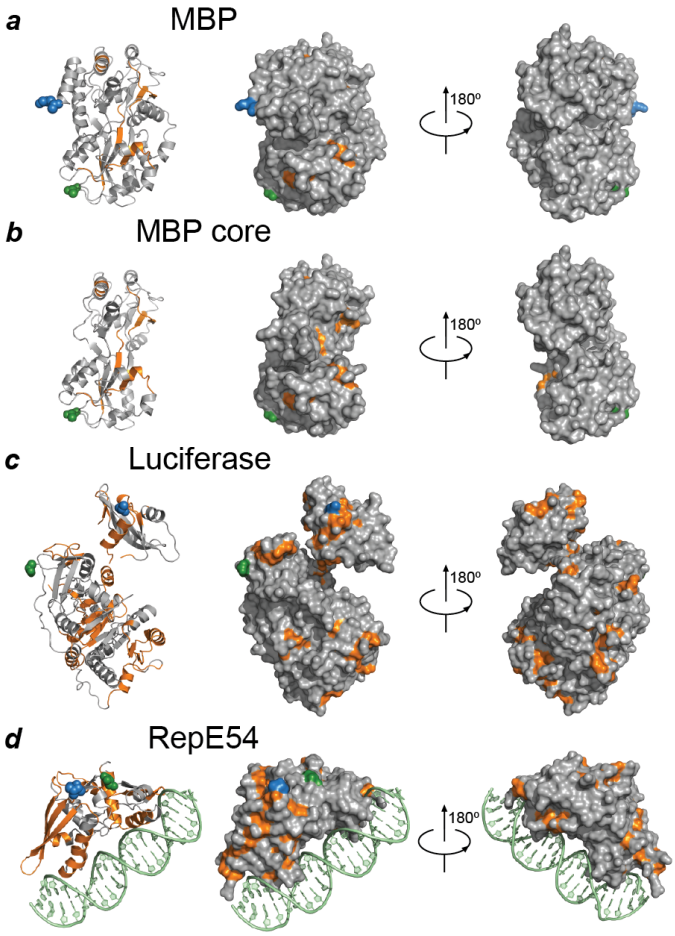

Extended Data Figure 4| Predicted peptides binding to DnaK for MBP, luciferase and RepE54. **a,** peptide-library trained predictions of DnaK-interacting peptide segments in the unfolded chain of MBP mapped in orange, using the algorithm introduced by Rüdiger *et. al.* [13] (PDB code: 1ANF). N-terminus marked green, C-terminus marked blue Surface representations of predicted peptides are restricted to their backbone atoms as their accessibility is central to canonical peptide binding of DnaK. **b,** Idem for MBP core structure. **c,** idem for firefly luciferase (PDB code: 1LCI) **d,** idem for RepE54 (PDB code: 1REP) including DNA ligand.

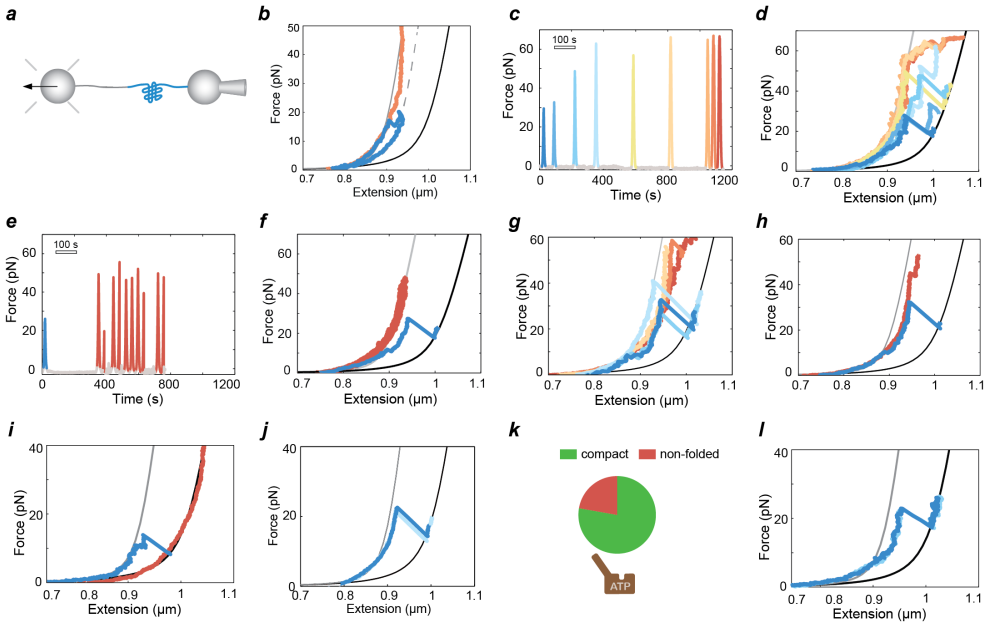

Extended Data Figure 5| Stabilization of folded structures by DnaK.
a, Schematic diagram of the set-up. DnaK and ADP were present in the experimental buffer from the start of the experiment. ***b,*** In the first stretching curve (blue), only C-terminal fragment of MBP was unfolded, and then force was immediately reduced to low force preventing further unfolding. After 3 min waiting at low force, subsequent stretching showed (orange) resistance to forced unfolding up to 50 pN. Experiments performed in 100 nM DnaK with 1 mM ADP loading buffer. **c,** Force acting on MBP is plotted versus time. Pulls (single stretching-relaxation cycles) on the same MBP molecule are followed by the increasing waiting periods at 0 pN, in the presence of 1 μM DnaK and 1 mM ADP loading buffer. **d,** Force-extension curves of MBP indicate increasing protection of partial folds against force (corresponding to panel c). Earlier pulls are in blue, latter in red. **e,** Force on MBP versus time. Identical buffer conditions as panels c and d. **f,** Force-extension curves of MBP indicate the stabilization of compact state of MBP (corresponding to panel e). First pull is highlighted in blue, subsequent pulls – in red. **g,** Force-extension curves of MBP in the presence of 100 nM DnaK and 1 mM ADP loading buffer. Blue: first stretching curves on different MBP molecules; orange and red: stretching curves after refolding and 3 min waiting at low force. **h-i,** MBP stretching and relaxation experiments in the presence of 1 μM DnaK with 100 μM ADP purified by HPLC were present. First stretching curves are shown in blue, stretching curves denoted in shades of red were acquired after 3 min waiting at low force. **j,** MBP stretching and relaxation in the presence of 100 nM DnaK mutant T199A and 1 mM ATP, which traps DnaK in the ATP state. **k,** Corresponding refolding probability (*N* = 18). **l,** Force-extension curves of MBP in the presence of 1 μM lid-truncated DnaK and 1 mM ADP loading buffer, after refolding and 3 min waiting at low force (N = 13).

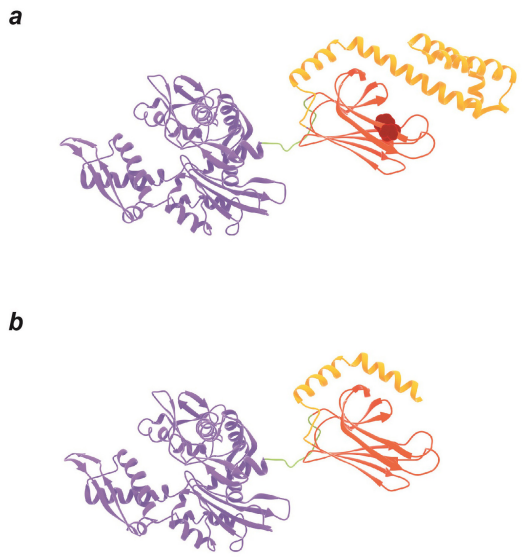

Extended Data Figure 6| DnaK mutant structures.
a, DnaK-V436F (termed groove-mutated) structure model highlighting in red spheres the location of the point mutation hindering access to its groove, resulting in a 38-fold reduction in peptide-binding affinity[25] (V436F substitution modeled onto PDB code: 2KH0). **b,** DnaK(2-538) (termed lid-truncated) structure (lid deletion modeled using 2KHO). The part of the lid that is still present in DnaK(2-538) interacts with the nucleotide binding domain in the ATP bound open conformation, which might be important for the mechanics of DnaK.

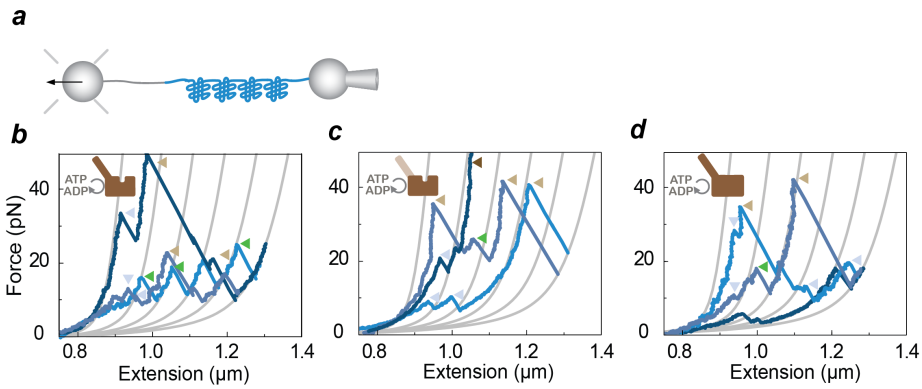

Extended Data Figure 7| 4MBP refolding in the presence of ATP and wild type or mutants of DnaK.
a, Scheme of the experiment. Stretching curves of 4MBP in the presence of ATP and wild-type DnaK (**b**), lid-truncated DnaK (**c**), and groove-mutated DnaK (**d**).

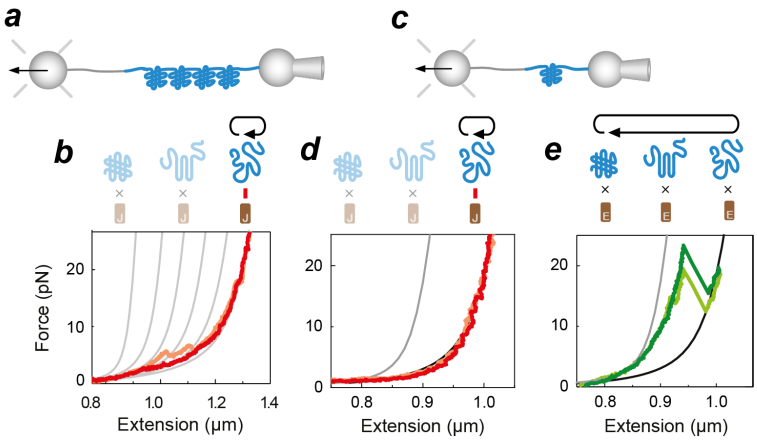

Extended Data Figure 8| MBP interaction with co-chaperone DnaJ and nucleotide exchange factor GrpE. a-b, 4MBP stretching in the presence of DnaJ. **a,** Scheme of the 4MBP experiment. **b,** A diagram of protein states and stretching curves of 4MBP with DnaJ. **c,** Scheme of the 1MBP experiment. **d,** MBP stretching in the presence of DnaJ. **e,** MBP stretching in the presence of GrpE.

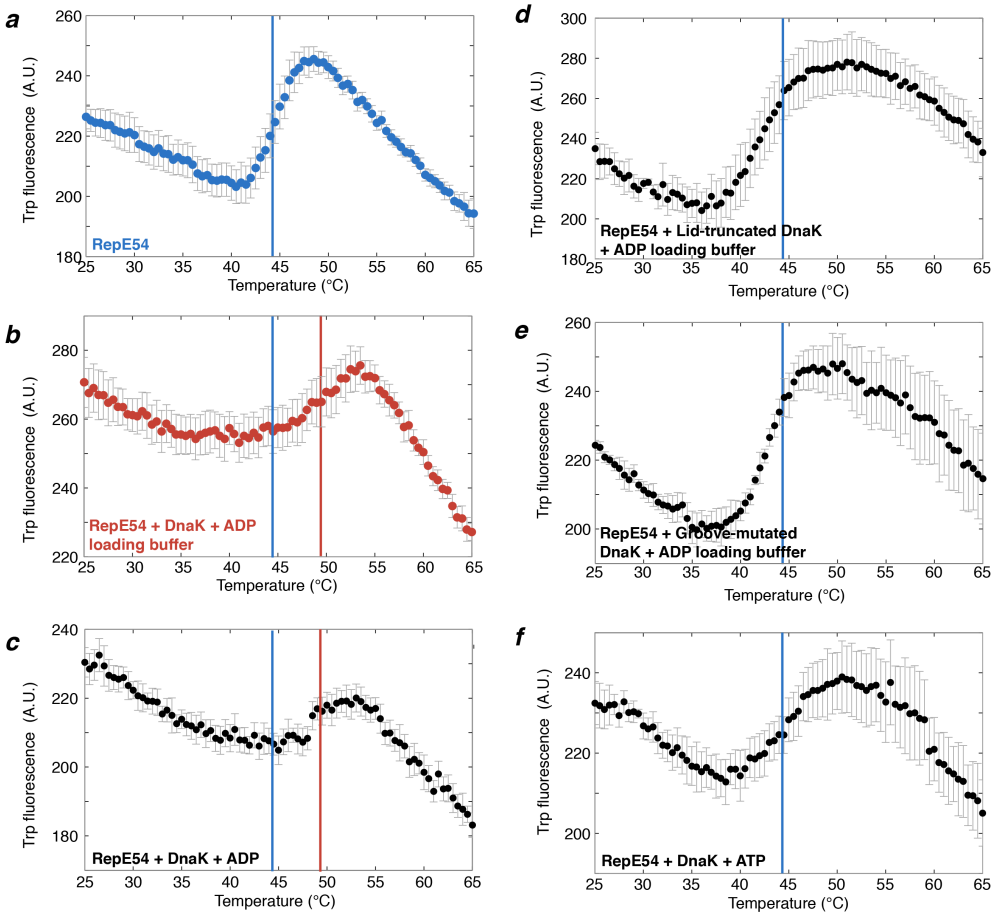

Extended Data Figure 9 | DnaK increases thermal stability of RepE54. a-f, Thermal denaturation curves of RepE54 as measured by tryptophan fluorescence in the absence (a) and presence of tryptophan free DnaK-W102F with ADP loading buffer (b), ADP (c), ATP (f) or lid-truncated (d) and groove-mutated tryptophan free DnaK (e). Vertical lines mark the apparent melting points of RepE54 only (blue) and DnaK-stabilized RepE54 (red). Error bars indicate the standard error of the mean over three replicates.

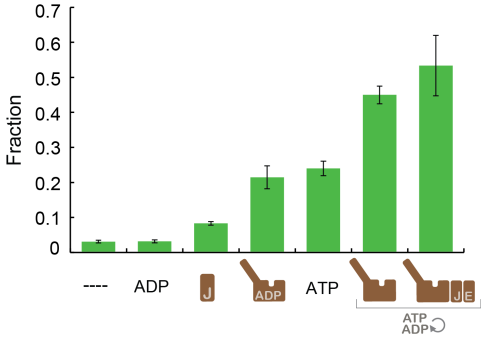

Extended Data Figure 10 | DnaK preserves enzyme activity. Bulk luciferase protection functional assay monitoring luciferase activity at 37°C in the absence or presence of nucleotides and chaperones as indicated. The active fraction of luciferase after 45 min from the start of temperature upshift from 0˚ to 37˚Cis shown. The experiment is performed in triplicates; error bars indicate the standard error of the mean.

Extended Data + Methods References

1 Rodriguez, F. *et al.* Molecular basis for regulation of the heat shock transcription factor sigma32 by the DnaK and DnaJ chaperones. *Molecular cell* **32**, 347-358, (2008).

2 Skowyra, D., Georgopoulos, C. & Zylicz, M. The E. coli dnaK gene product, the hsp70 homolog, can reactivate heat-inactivated RNA polymerase in an ATP hydrolysis-dependent manner. *Cell* **62**, 939-944, (1990).

3 Kirschke, E., Goswami, D., Southworth, D., Griffin, P. R. & Agard, D. A. Glucocorticoid receptor function regulated by coordinated action of the Hsp90 and Hsp70 chaperone cycles. *Cell* **157**, 1685-1697, (2014).

4 Sharma, S. K., De los Rios, P., Christen, P., Lustig, A. & Goloubinoff, P. The kinetic parameters and energy cost of the Hsp70 chaperone as a polypeptide unfoldase. *Nat Chem Biol* **6**, 914-920, (2010).

5 Schroder, H., Langer, T., Hartl, F. U. & Bukau, B. DnaK, DnaJ and GrpE form a cellular chaperone machinery capable of repairing heat-induced protein damage. *The EMBO journal* **12**, 4137-4144, (1993).

6 Calloni, G. *et al.* DnaK functions as a central hub in the E. coli chaperone network. *Cell reports* **1**, 251-264, (2012).

7 Mayer, M. P. & Bukau, B. Hsp70 chaperones: cellular functions and molecular mechanism. *Cellular and molecular life sciences : CMLS* **62**, 670-684, (2005).

8 Frydman, J., Nimmesgern, E., Ohtsuka, K. & Hartl, F. U. Folding of nascent polypeptide chains in a high molecular mass assembly with molecular chaperones. *Nature* **370**, 111-117, (1994).

9 Hartl, F. U. & Hayer-Hartl, M. Molecular chaperones in the cytosol: from nascent chain to folded protein. *Science* **295**, 1852-1858, (2002).

10 Tyedmers, J., Mogk, A. & Bukau, B. Cellular strategies for controlling protein aggregation. *Nature reviews. Molecular cell biology* **11**, 777-788, (2010).

11 Warrick, J. M. *et al.* Suppression of polyglutamine-mediated neurodegeneration in Drosophila by the molecular chaperone HSP70. *Nature genetics* **23**, 425-428, (1999).

12 Zhu, X. *et al.* Structural analysis of substrate binding by the molecular chaperone DnaK. *Science (New York, N Y)* **272**, 1606-1614, (1996).

13 Rudiger, S., Germeroth, L., Schneider-Mergener, J. & Bukau, B. Substrate specificity of the DnaK chaperone determined by screening cellulose-bound peptide libraries. *The EMBO journal* **16**, 1501-1507, (1997).

14 Szabo, A. *et al.* The ATP hydrolysis-dependent reaction cycle of the Escherichia coli Hsp70 system DnaK, DnaJ, and GrpE. *Proceedings of the National Academy of Sciences of the United States of America* **91**, 10345-10349, (1994).

15 Qi, R. *et al.* Allosteric opening of the polypeptide-binding site when an Hsp70 binds ATP. *Nature structural & molecular biology* **20**, 900-907, (2013).

16 Kityk, R., Kopp, J., Sinning, I. & Mayer, M. P. Structure and dynamics of the ATP-bound open conformation of Hsp70 chaperones. *Molecular cell* **48**, 863-874, (2012).

17 Schlecht, R., Erbse, A. H., Bukau, B. & Mayer, M. P. Mechanics of Hsp70 chaperones enables differential interaction with client proteins. *Nature structural & molecular biology* **18**, 345-351, (2011).

18 Smock, R. G., Blackburn, M. E. & Gierasch, L. M. Conserved, disordered C terminus of DnaK enhances cellular survival upon stress and DnaK in vitro chaperone activity. *The Journal of biological chemistry* **286**, 31821-31829, (2011).

19 Buchberger, A., Schroder, H., Hesterkamp, T., Schonfeld, H. J. & Bukau, B. Substrate shuttling between the DnaK and GroEL systems indicates a chaperone network promoting protein folding. *J Mol Biol* **261**, 328-333, (1996).

20 Marcinowski, M. *et al.* Substrate discrimination of the chaperone BiP by autonomous and cochaperone-regulated conformational transitions. *Nature structural & molecular biology* **18**, 150-158, (2011).
21 Bechtluft, P. *et al.* Direct observation of chaperone-induced changes in a protein folding pathway. *Science* **318**, 1458-1461, (2007).
22 Mashaghi, A. *et al.* Reshaping of the conformational search of a protein by the chaperone trigger factor. *Nature* **500**, 98-101, (2013).
23 Wang, M. D., Yin, H., Landick, R., Gelles, J. & Block, S. M. Stretching DNA with optical tweezers. *Biophysical journal* **72**, 1335-1346, (1997).
24 Sikor, M., Mapa, K., von Voithenberg, L. V., Mokranjac, D. & Lamb, D. C. Real-time observation of the conformational dynamics of mitochondrial Hsp70 by spFRET. *The EMBO journal* **32**, 1639-1649, (2013).
25 Mayer, M. P. *et al.* Multistep mechanism of substrate binding determines chaperone activity of Hsp70. *Nature structural biology* **7**, 586-593, (2000).
26 Gamer, J. *et al.* A cycle of binding and release of the DnaK, DnaJ and GrpE chaperones regulates activity of the Escherichia coli heat shock transcription factor sigma32. *The EMBO journal* **15**, 607-617, (1996).
27 Ishiai, M., Wada, C., Kawasaki, Y. & Yura, T. Replication Initiator Protein Repe of Mini-F Plasmid - Functional-Differentiation between Monomers (Initiator) and Dimers (Autogenous Repressor). *Proceedings of the National Academy of Sciences of the United States of America* **91**, 3839-3843, (1994).
28 Kellner, R. *et al.* Single-molecule spectroscopy reveals chaperone-mediated expansion of substrate protein. *Proceedings of the National Academy of Sciences of the United States of America* **111**, 13355-13360, (2014).
29 Nunes, J. M., Mayer-Hartl, M., Hartl, F. U. & Muller, D. J. Action of the Hsp70 chaperone system observed with single proteins. *Nature communications* **6**, 6307, (2015).
30 Rutherford, S. L. & Lindquist, S. Hsp90 as a capacitor for morphological evolution. *Nature* **396**, 336-342, (1998).
31 Li, Z., Hartl, F. U. & Bracher, A. Structure and function of Hip, an attenuator of the Hsp70 chaperone cycle. *Nature structural & molecular biology* **20**, 929-935, (2013).
32 Grimshaw, J. P., Jelesarov, I., Schonfeld, H. J. & Christen, P. Reversible thermal transition in GrpE, the nucleotide exchange factor of the DnaK heat-shock system. *The Journal of biological chemistry* **276**, 6098-6104, (2001).
33 Buchberger, A., Valencia, A., McMacken, R., Sander, C. & Bukau, B. The chaperone function of DnaK requires the coupling of ATPase activity with substrate binding through residue E171. *The EMBO journal* **13**, 1687-1695, (1994).
34 Packschies, L. *et al.* GrpE accelerates nucleotide exchange of the molecular chaperone DnaK with an associative displacement mechanism. *Biochemistry-Us* **36**, 3417-3422, (1997).
35 Pellecchia, M., Szyperski, T., Wall, D., Georgopoulos, C. & Wuthrich, K. NMR structure of the J-domain and the Gly/Phe-rich region of the Escherichia coli DnaJ chaperone. *J Mol Biol* **260**, 236-250, (1996).
36 Li, J., Qian, X. & Sha, B. The crystal structure of the yeast Hsp40 Ydj1 complexed with its peptide substrate. *Structure* **11**, 1475-1483, (2003).
37 Harrison, C. J., Hayer-Hartl, M., Di Liberto, M., Hartl, F. & Kuriyan, J. Crystal structure of the nucleotide exchange factor GrpE bound to the ATPase domain of the molecular chaperone DnaK. *Science* **276**, 431-435, (1997).
38 Mayer, M. P. Gymnastics of Molecular Chaperones. *Molecular cell* **39**, 321-331, (2010).
39 Bertelsen, E. B., Chang, L., Gestwicki, J. E. & Zuiderweg, E. R. Solution conformation of wild-type E. coli Hsp70 (DnaK) chaperone complexed with ADP and substrate. *Proceedings of the National Academy of Sciences of the United States of America* **106**, 8471-8476, (2009).

Acknowledgements

Work in the laboratory of S.J.T. is part of the research programme of the Stichting voor Fundamenteel Onderzoek der Materie (FOM), which is financially supported by the Nederlandse Organisatie voor Wetenschappelijke Onderzoek (NWO). We thank M. M. Naqvi for performing control experiments, M. Avellaneda for help with preparing protein structure illustrations, and T. Shimizu, E. Garnett and F. Huber for critical reading of the manuscript.

Author Information

The authors declare no competing financial interests. Correspondence and requests for materials should be addressed to S.J.T. (tans@amolf.nl).

Author contributions

AM, SB, DM, MM, GK, BB, and ST conceived and designed the research; BZB and DM designed and purified the MBP protein constructs; AM and SB performed the optical tweezers experiments; BZB, GK, AW, MM purified the DnaK system chaperones and DnaK mutants; AW performed the bulk RepE54 assays; RK performed the bulk luciferase assays; AM, SB, AW, and ST analyzed the data; and AM, SB, DM, MM, GK, BB, and ST wrote the paper.